Applied Surface Science 403 (2017) 356–361

Contents lists available at ScienceDirect

Applied Surface Science

journal homepage: www.elsevier.com/locate/apsusc

Full Length Article

Impact of self-assembled monolayer assisted surface dipole modulation of PET substrate on the quality of RF-sputtered AZO film

Thieu Thi Tien Vo[a,b], K.P.O. Mahesh[a], Pao-Hung Lin[c], Yian Tai[a,*]

[a] Department of Chemical Engineering, National Taiwan University of Science and Technology, Taipei 10607, Taiwan
[b] Faculty of Chemical Engineering and Food Technology, Ba Ria-Vung Tau University, Vung Tau, Vietnam
[c] Department of Electronic and Computer Engineering, National Taiwan University of Science and Technology, Taipei 10607, Taiwan

ARTICLE INFO

Article history:
Received 1 September 2016
Received in revised form
28 December 2016
Accepted 16 January 2017
Available online 21 January 2017

Keywords:
Self assembled monolayers (SAMs)
Aluminum doped zinc oxide (AZO)
RF sputtering
Polyethylene terephthalate (PET)
Surface dipole

ABSTRACT

In this study, we fabricated the electron donating/withdrawing group functionalized organosilane self-assembled monolayers (SAMs) on transparent polyethylene terephthalate (PET) flexible substrate followed by the deposition of aluminum doped zinc oxide (AZO) using RF magnetron sputtering at room temperature. The effect of different SAMs on transparent PET substrates and AZO films were studied by contact angle (CA), X-ray photoelectron spectroscopy (XPS), Atomic force microscopy (AFM), X-ray diffraction (XRD), Field-Emission scanning electron microscope (FE-SEM), Hall measurement and UV–vis spectroscopy (UV–vis). The results presented that the surface dipole (i.e. electron-donating/withdrawing) of different SAMs functionalized PET substrates affected the quality of the AZO films which deposited on top of them. The crystallinity, the charge mobility, and the carrier concentration of the AZO improved when the film was deposited on the PET functionalized with electron donating group, which was possibly due to favored interaction between electron donating group and Al ions.

1. Introduction

Transparent conducting oxide (TCO) films have been widely studied for transparent and flexible device applications such as liquid crystal displays, plasma display panels, electronic paper displays, organic light-emitting diode, solar cells, touch panels, gas sensor and other optoelectronic devices [1–3]. Recently aluminum doped zinc oxide (AZO) films have received more attention due to its low electrical resistivity, high optical transmittance in the visible and near-infrared (IR) regions (Bandgap = 3.3–3.9 eV), high thermal stability, non-toxic characteristics, low-cost and abundant source [4–8].

In recent years, the flexible electronics has attracted much attention due to its potential advantages over light weight, smaller in dimensions, space saving, foldable and bendable [9,10]. The most important advantages of flexible plastic substrates are economically cheaper, inexpensive roll to roll processing and simple ink-jet printing on substrate for electronic devices. Hence it is foremost important to work on the deposition of oxide thin film on plastic substrates to replace solid substrates.

In this sense, poly-ethylene terephthalate (PET) has become an ideal candidate as a substrate material for flexible electronics. PET is a vastly used thermoplastic polymer in commercial due to its high tensile and impact strength, adequate CO_2 retention, chemical resistance, optical clarity, processability, design flexibility, and low-cost [9,11,12].

For the fabrication of AZO film on PET, it is important to consider the thermal stability of polymer materials that could degrade at below 180 °C, therefore the low temperature process is required for the deposition of AZO film on polymer substrate. There are several works have been reported for ZnO:Al (AZO) films deposited on the flexible substrates using different deposition methods [13–16]. Among these, the simple solution process and RF magnetron sputtering are the preferred methods owing to their low temperature processing. Variety of solution processes have used to obtain AZO film with good optoelectronic properties [17,18]. However, using Al as a dopant in the aqueous solution (in the form of Al ions) affects the ZnO crystal growth and also the existence of trace amount of $Al(OH^{4-})$ affects the morphology of AZO film [19]. Further, it is very difficult to avoid the impurities during the formation of AZO film. Those problems are hindered to achieve a good crystalline, dense and less resistive AZO thin film. In RF magnetron process, ZnO and Al_2O_3 targets are used to grow AZO film. Therefore, it is possible to achieve high pure, uniform, smooth and highly crystalline AZO thin films that could deposit over large area substrates. However, using

* Corresponding author.
E-mail address: ytai@mail.ntust.edu.tw (Y. Tai).

http://dx.doi.org/10.1016/j.apsusc.2017.01.156
0169-4332/

RF magnetron sputtering, the low temperature process is not in favor of depositing high quality films and the resistivity of AZO films is quite high due to low surface energy and high surface roughness of PET film.

It is well known that the physical properties of the substrate surface affect the crystallinity of the thin film deposit on it. Those properties including surface energy, lattice constant, and surface dipole moment. To deposit high crystalline AZO on PET with low temperature process, a possible approach is to modulate those properties of the substrate to optimize the surface condition.

In our previous work [20,21], we reported the surface modification of glass substrate by utilizing self-assembled monolayers (SAMs). The SAMs with different alkyl chains varies the surface energies of glass substrate without changing the surface dipole moment. The improvement in crystallinity obtained for the AZO films that were grown on glass substrate modified with longer alkyl chain SAM. However, in the case of PET, it is not possible to further reduce the surface energy of the polymer by utilizing SAMs, since PET possesses lower surface energy. Moreover, the PET is not a highly crystalline material, using SAM could not improve the lattice mismatch between PET and AZO. However, we could attempt to use SAMs with functional groups of different polarity (electron donating or withdrawing nature) to modulate the affinity between PET surface and AZO species, which might lead to improvement in crystallinity of AZO film and thus further enhancing its electrical properties even at low temperature processing. It is noteworthy that to the best of our knowledge, only very few works have been reported on the fabrication of SAMs on polymer substrates [22,23].

In the present work, AZO films were deposited on different organosilane SAMs modified PET substrate using RF magnetron sputtering at room temperature. SAMs with electron donating functional group, —NH_2, and electron withdrawing group, —CN, were applied. The crystallinity, electrical and optical properties of the AZO film fabricated on different SAMs modified PET were studied, and the results revealed that those AZO film properties are correlated with the surface dipole of the PET substrates.

2. Experiment

2.1. Materials

PET substrates were kindly supplied by Teijin DuPont Films and were cut into 2 cm x 2 cm pieces. 3-cyanopropyltriethoxysilane (–CN-SAM, 95%, Sigma-Aldrich) and 3-aminopropyltrimethoxysilane (–NH_2 SAM, 97%, Acros Organics) were used as received. Acetone, 2-propanol and *n*-decane were purchased from Acros Organics and were either of semiconductor or reagent grade (99%).

2.2. Surface modification of PET substrate using organosilane SAMs

The surfaces of PET substrates were cleaned in an ultrasonic bath for 15 min each with detergent, deionized (DI) water, acetone and 2-propanol (IPA) followed by blown dried with N_2. In order to increase the concentration of hydrophilic groups such as —COOH or —OH on the surface of the PET substrate, the cleaned substrates were exposed to UV–Ozone irradiation. After that, the substrates were immersed into 1 mM SAM/decane solutions for 24 h at 25 °C. Then, the SAM modified UV–Ozone irradiated PET (uv-PET) substrates were rinsed with ethanol and blown dried by N_2. The reaction mechanism for the formation of organosilane SAMs on uv-PET are shown in Fig. S1. In this work, two different types of SAMs (–NH_2 and —CN SAMs) were used to modify the surface of uv-PET substrates (uv-PET).

Table 1
The water contact angles of pristine PET, uv-PET, and —CN and —NH_2 SAMs modified uv-PET substrates.

Samples	Contact angle (deg.)
Pristine PET	74.9 ± 2.2
uv-PET	18.9 ± 5.3
–NH_2/PET	60.1 ± 1.9
–CN/PET	57.8 ± 1.1

2.3. AZO thin film fabrication

AZO thin films were deposited on SAMs modified uv-PET substrates using RF sputtering at room temperature. A 2 inches ceramic target (ZnO/Al_2O_3 = 98:2 wt%, 99.99%, Cathay Advanced Materials Limited) was loaded on the cathode, using a plasma power of 20 W, the distance between the target and substrate stage was adjusted from 30 to 70 mm. The sputter chamber was evacuated at around 8.0×10^{-7} Torr by using a turbomolecular pump and then back filled with Ar gas to reach the desired working pressure (2.0×10^{-3}–8.0×10^{-3} Torr). A shutter was placed immediately above the sample to ensure that the deposition would start only after the equilibrium point would be reached. The deposition time for each sample was 60 min. With the deposition rate of ~5 nm/min, the thicknesses of all the AZO films on PET were ~280 nm.

2.4. Characterization

The optical properties were investigated using UV–vis spectroscopy (Jasco-V-670). All the spectra were normalized with respect to the actual film thicknesses. Contact angle was measured using water contact angle (CA) meter (Creating Nano Technologies Inc.). Crystallinity of the samples was investigated by X-ray diffraction (XRD, PANalyticalX'Pert PRO) and the selected area electron diffraction (SAED) was studied using a Philips Tecnai FE30 field-emission-gun transmission electron microscope (TEM) equipped with SAED attachment. The surface roughness and morphology of the devices were probed by atomic force microscopy (AFM; Digital Nanoscope IIIA) using the tapping mode. Surface morphology of samples was studied using Field-Emission Scanning Electron Microscopy (FESEM, JOEL6400). Nanostructures were investigated using X-ray photoelectron spectroscopy (XPS, VG ESCA Scientific Theta Probe system using an Al Kα source at 1486.6 eV with an x-ray probe spot size of 400 μm). The electrical properties were measured using Ecopia HMS-3000 Hall measurement and four-point probe instruments.

3. Results and discussion

3.1. SAMs modified uv-PET substrate

Table 1 shows the DI water contact angles (CAs) of pristine PET, UV-Ozone treated PET (uv-PET) and SAMs with electron withdrawing and donating groups (–CN and —NH_2) modified uv-PET substrates. The contact angles (CAs) of pristine PET and uv-PET substrates are 74.9° and 18.9°, respectively due to the increment of hydrophilic groups such as hydroxyl and carboxylic groups on the surface of uv-PET substrate. Whereas the water CAs of SAMs modified uv-PET substrates were three folds higher than that of uv-PET, which suggested that the SAMs were successfully fabricated on uv-PET surfaces. The UV treatment helped to increase the hydrophilic groups on the PET substrate and the presence of higher concentrations of hydrophilic groups on PET substrate can easily react with more number of Si-$(OCH_3)_3$ groups of the SAM molecules. The pos-

sible mechanism of the silane-SAMs grown on uv-PET substrate is illustrated in supplementary information (SI) and Fig. S1.

The critical surface tensions of uv-PET substrates modified by SAMs with —CN and —NH_2 functional groups, were deduced from Zisman plot [24] as shown in Table S1 in SI. It was found that there is no considerable difference in the surface tensions of the uv-PET and these SAMs modified uv-PET substrates. Because the uv-PET substrate have low surface tension around 40 mN/m and SAMs also have low surface tensions between 25 and 40 mN/m, which could not help to modulate the PET surface tension after modified by SAMs.

Fig. 1 shows the XPS spectra of —CN and —NH_2 SAMs modified uv-PET substrates. The N 1s peaks of —CN (Fig. 1a) and —NH_2 (Fig. 1b) are presented at 398.5 eV and 399.5 eV, respectively. As in —CN group, the nitrogen bind the carbon atom with triple-bond, resulting in higher tendency of electron donating from C to N as compared with that of nitrogen in —NH group. Therefore, it is rational that the N1s in —CN has lower binding energy than that of —NH_2. The Si 2p core level peaks of —CN and —NH_2 SAMs (Fig. 1c and d, respectively) appeared at around 102.5 eV which are in good agreement with the reported values (102–102.5 eV) for siloxane molecules [25]. The peak areas of Si 2p, and N 1s were normalized as shown in Table S2 in SI. These results are also consistent with the molecular structures of the utilized SAMs (The ratio of Si and N are 1:1 for both SAMs). It is indicated that the UV–Ozone pre-treatment on PET substrates favors a denser packing of silane molecules by the self-assembly process on the uv-PET surfaces.

The work functions of these SAMs modified uv-PET substrate were determined by AC2 as shown in Table 2. AC2 is an instrument for photoelectron spectroscopy at atmospheric pressure, which is an open counter equipped with the UV source. The open counter is a unique electron detector that can be operated in ambient. The work functions of uv-PET modified by SAMs depend on the nature of the functional groups present in the SAMs. It is clearly found that the work functions of —CN SAM modified uv-PET increased due to the electron withdrawing nature of —CN whereas the —NH_2 SAM modified substrate decreased due to the presence of electron donating —NH_2.

Table 2
The work functions of pristine uv-PET and —CN and —NH_2 SAMs modified uv-PET substrates.

Samples	Work function (eV)
uv-PET	5.45
–CN/uv-PET	5.83
–NH_2/uv-PET	5.02

The UV transmittance measurements were conducted for studying the optical properties of unmodified and SAMs-modified uv-PET substrates. The transmittance spectra of SAMs-modified uv-PET substrate are almost similar to the unmodified uv-PET substrates and these average transmittance is about 90% in the visible region as shown in Fig. S3 in SI. These results indicate that the fabrication of SAMs do not induce any structural changes on the surface of PET substrates and thus, it does not influence the optical properties of uv-PET substrates.

3.2. AZO film on PET substrate

PET is a polymer substrate which is sensitive to heat. From this aspect, the condition of deposition of AZO film on PET substrate preferred for RF magnetron sputtering, are low power and room temperature (RT). All experimental results are the average of at least 5 samples. The thickness of pristine, and —CN and —NH_2

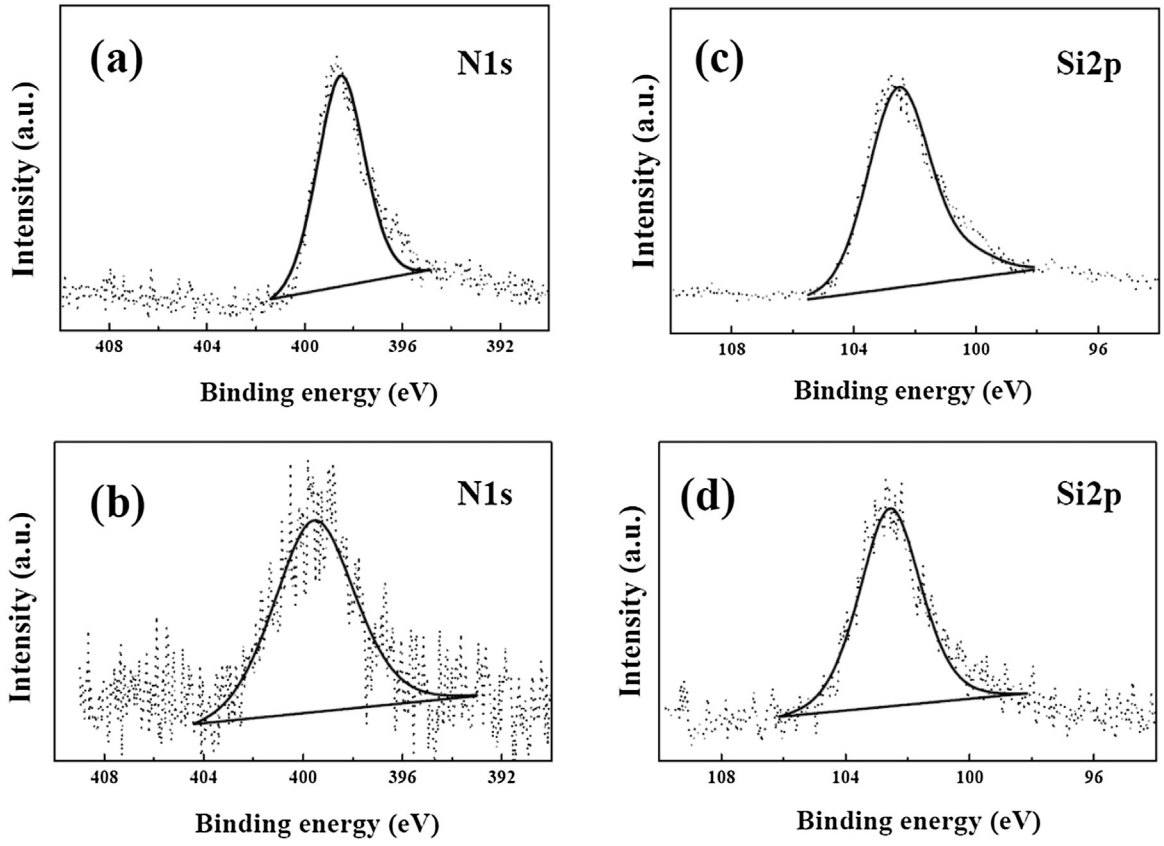

Fig. 1. N1s and Si2p XPS spectra of —CN and —NH_2 SAMs modified uv-PET substrate.

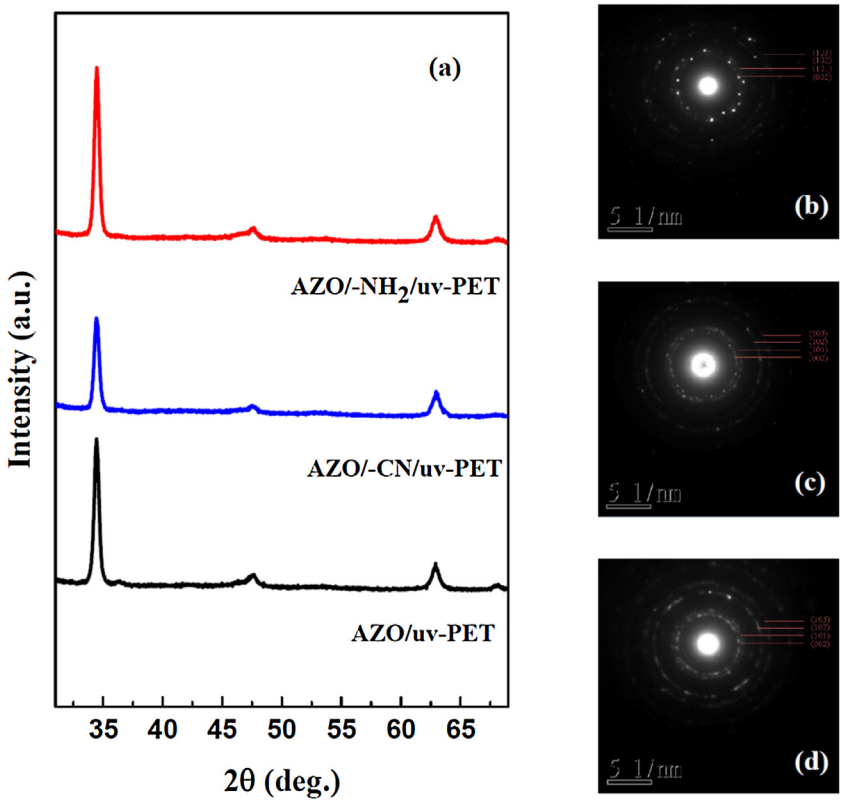

Fig. 2. XRD patterns of AZO films deposited on (a) uv-PET, and –CN and —NH_2 SAMs modified uv-PET substrate and SAED patterns of AZO films deposited on (b) SAMs with electron donating functional group (–NH_2), (c) pristine uv-PET and (d) SAMs with electron withdrawing functional group (–CN).

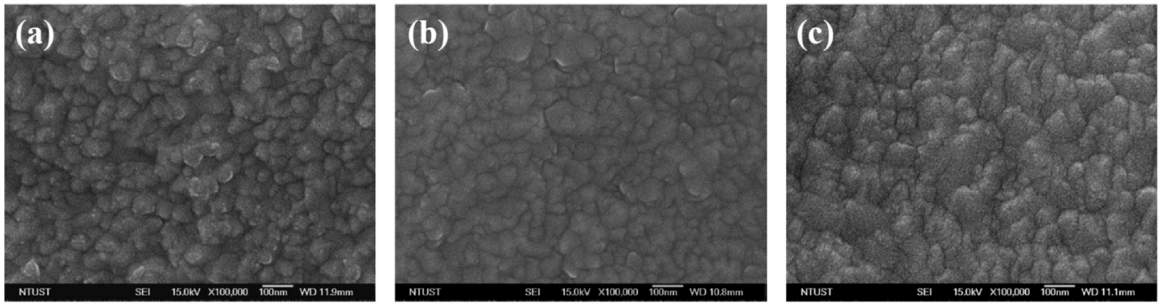

Fig. 3. SEM images of AZO films deposited on a) pristine uv-PET, and b) —CN and c) —NH_2 SAMs modified uv-PET for 60 min.

modified AZO films deposited on PET are 276 ± 15, 274 ± 17, and 279 ± 18 nm, respectively.

The XRD patterns for AZO films deposited on uv-PET, —CN and —NH_2 SAMs modified uv-PET substrates revealed a strong 2θ peak at 34.4° and other weak 2θ peaks appeared at 47.5° and 62.8°, which correspond to the (002), (102) and (103) orientations, respectively as shown in Fig. 2a. The XRD result indicates that all the AZO films were polycrystalline with a preferential (002) orientation and having a well-defined *c*-axis orientation perpendicular to the substrate surface. However, the (002) peak areas of AZO films deposited on SAMs modified uv-PET substrates were quite different as compared to the AZO film deposited on uv-PET substrate as shown in Fig. 2a. The degree of crystallinity of uv-PET substrate could be altered by modifying the substrate with different functional group SAMs. The SAED results further confirm that the changes in crystallinity of the AZO films fabricated using different SAMs on uv-PET substrates as shown in Fig. 2b–d. Comparing with the AZO deposited on pristine uv-PET (Fig. 2c) The SAMs with electron donating functional group (–NH_2) enhanced the crystallinity of AZO film (Fig. 2b), whereas electron withdrawing functional group (–CN) reduced the crystallinity of AZO film (Fig. 2d).

Fig. 3 shows the SEM images of AZO films deposited on uv-PET, —CN and —NH_2 SAM modified uv-PET substrates at 60 min. Fig. 3 shows that the AZO crystals are grown with more discontinuous grain boundaries on the uv-PET (Fig. 3a) and —CN (Fig. 3b) modified uv-PET substrates when compared with —NH_2 SAM modified PET substrate (Fig. 3c), which the grain sizes of AZO crystals are larger with very tightly packed grains. This might be due to the electron donating nature of —NH_2 SAM that enhances the ionic interaction between PET substrates and AZO film. The surface tensions of uv-PET, —CN, and —NH_2 SAM modified uv-PET substrates were calculated as 43.3, 37.9 and 41.1 mN/m, respectively. These surface tensions are not high enough for the AZO films to wet the substrate and the interface width of the growing surface increases with depo-

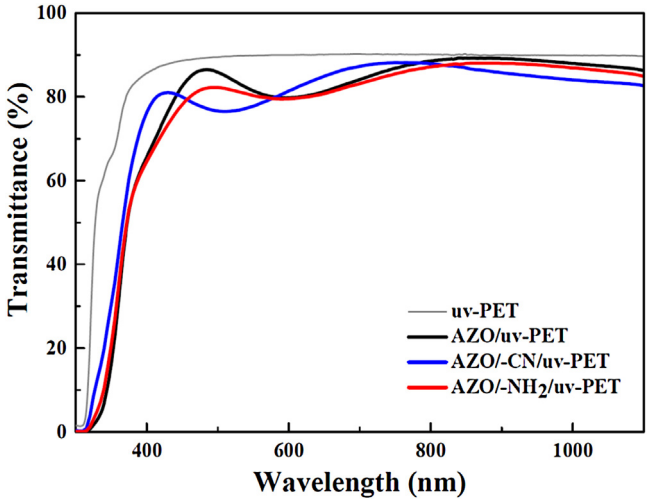

Fig. 4. UV-vis transmittance spectra of AZO films deposited on uv-PET, and —CN and —NH_2 SAMs modified uv-PET substrate.

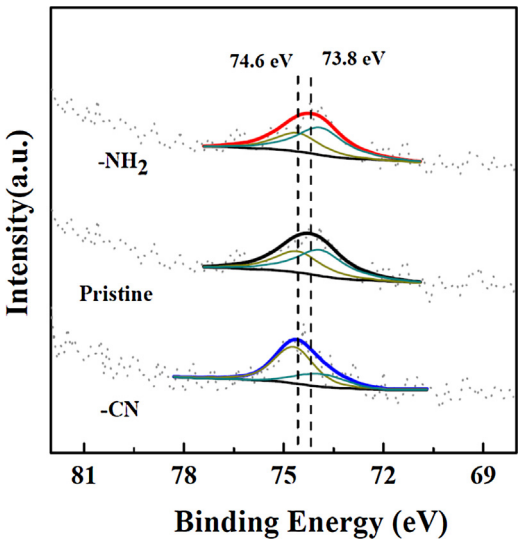

Fig. 5. Al 2p core level XPS spectra of AZO films deposited on uv-PET, and —CN and —NH_2 SAMs modified uv-PET substrate.

sition time, which was referred as so-called Islands growth mode (or Volmer-Weber mode) [20]. This result is consistent with the XRD data as shown in Fig. 2a.

The transmittance spectra of AZO thin films deposited on uv-PET substrates modified with —CN and —NH_2 SAMs are shown in Fig. 4. The spectrum of bare uv-PET is also offered as reference. The average transmittance in the visible wavelength region is about 85% for all the films, indicating that these organosilane SAMs do not have a significant effect on the transparency of the AZO films in the visible region.

The electrical properties of AZO thin films deposited on different SAMs modified uv-PET substrates are investigated by a Hall measurement system as given in Table 3. The deposition conditions were kept identical for pristine uv-PET, and both —CN and —NH_2 SAMs modified uv-PET substrates. The electrical properties are mainly affected by carrier concentration. The resistivity increased with decreasing the carrier concentration for AZO film deposited on electron withdrawing —CN-SAM modified uv-PET substrate. On the other hand, the resistivity decreased with increasing the carrier concentration for AZO films deposited on the electron donating —NH_2 SAMs modified uv-PET substrate. This is attributed to the Al substitution in ZnO lattice ratio that will be discussed later. In addition, the carrier mobility also affected the electrical properties of the AZO films to some extent. The Hall measurement results are consistent with the XRD results, viz the carrier mobility is related to the crystallinity of the AZO film, i.e. the better the crystallinity, the higher the mobility. The minimum resistivity (1.1×10^{-3} Ω/cm) corresponding to sheet resistance 40.1 Ω/□was obtained from AZO film deposited on —NH_2 SAM modified uv-PET substrate. This resistance is comparable even slightly better than that of the commercially available AZO/PET films ($R_s \approx 60$–90 Ω/□, %T ≈ 80, thickness ~300 nm).

Fig. 5 shows Al 2p core level XPS spectra of AZO films deposited on pristine and —CN and —NH_2 SAMs modified uv-PET substrate, which were deconvolved into two components located at 73.8 eV (dark cyan lines) and 74.6 eV (dark yellow lines). The low binding energy peak centered at 73.8 eV is attributed to the Al-O bonding in ZnO lattice and the high binding energy peak centered at 74.6 eV is attributed to Al-O bonding in Al_2O_3 segregated at the grain boundaries. The ratio of Al substitution in ZnO lattice to total Al were found to be increased for AZO films deposited on —NH_2 SAM and decreased for AZO film deposited on —CN SAM compared to that of AZO film on uv-PET as shown in Fig. 5. This result indicates that the amount of Al^{3+} ion substituted into Zn^{2+} ion increased for the substrate surface modified by the —NH_2 functional group, possibly due to the attraction between positively charged Al^{3+} and electron donating functional groups, and decreased for the substrate surface modified by the electron withdrawing functional groups due to the weak interaction between Al^{3+} and —CN. The carrier concentration and the resistivity of AZO film on uv-PET are highly affected by Al concentration in ZnO lattice and also the effect of organosilane SAMs with different functional groups. The ratios of Al in ZnO lattice to total Al were calculated from the measured peak areas as presented in Table 4.

Table 4
Ratio of the amount of Al in AZO lattice to total amount of Al obtained by XPS spectra.

Samples	Ratio of Al in ZnO lattice to total Al
AZO/-NH_2/uv-PET	0.65
AZO/uv-PET	0.59
AZO/-CN/uv-PET	0.30

3.3. Discussion

Organosilanes based self-assembled monolayer are extensively used in variety of applications due to its easy reaction with the surface of metal or metal oxides. [26–28] In this study, two different (–NH_2 and —CN) functionalized organosilanes are used for the formation of self-assembled monolayer on the UV-Ozone treated PET substrate. The head group i.e., Si-$(OCH_3)_3$ of both —CN and —NH_2 SAMs could easily react with hydroxyl or carboxylic groups of the uv-PET substrate. The tail end of the —NH_2 SAM possesses electron donating group that could have good interaction with positively charged Al^{3+} or Al^{2+} ion from the aluminum precursor. A strong and uniform dipoles have formed between the PET substrate and AZO thin film due to the electrostatic interaction generated by electron donating (–NH_2) group of SAM molecule [29,30]. Moreover, during sputtering, a lone pair electrons in the —NH_2 SAM could possible to have an ionic bonding with Al ions and these Al ions may diffuse into the ZnO cubic crystal in the AZO film. Further, these Al^{3+} ions replaced Zn^{2+} in the ZnO lattice to form the high crystalline AZO film. In the case of the electron withdrawing group (–CN) of SAM molecule, there is a repulsive force formed between the —CN and the Al^{3+} ion during the deposition of AZO film that lead to hinder the Al atom to replace the Zn in ZnO lattice. Moreover, some of the Al atoms segregated on the grain boundaries to form AlO bonding

Table 3
Electrical properties of AZO film deposited on uv-PET, and —CN and —NH_2 SAMs modified uv-PET substrate.

Samples	Carrier Concentration (x10^{20} cm^{-3})	Hall Mobility (cm^2 V^{-1} s^{-1})	Resistivity (x10^{-3} Ω cm)
AZO/uv-PET	10.11 ± 0.80	2.82 ± 0.66	2.29 ± 0.48
AZO/-CN/uv-PET	7.46 ± 0.25	2.73 ± 0.38	3.12 ± 0.57
AZO/-NH_2/uv-PET	14.74 ± 2.38	3.78 ± 0.40	1.12 ± 0.16

and both Al and Zn atoms shared the same lattice that might be responsible for the electron scattering and obtained a very poor quality AZO film. The replacement of Zn by Al atom in ZnO lattice and the segregation of Al atom on the ZnO grain boundaries are responsible for the reduction and enhancement of electrical resistance of AZO film, respectively. The SAM modified PET substrate with surface dipole (electron donating group) substantiate the formation of high crystalline and low electrical resistivity of AZO film grown at low temperature.

4. Conclusion

Organosilane based self-assembled monolayers were successfully directly grown on UV-Ozone treated PET substrate by —CN and —NH_2/n-decane solution without using buffer layer followed by the deposition of Al-doped ZnO thin films on SAM-PET substrate at room temperature using RF magnetron sputtering. The optical transmittance of both SAMs modified AZO films achieved 85% of transmittance in visible wavelength region. The functional groups of the SAMs played an important role in the structural behaviors and resistivity of uv-PET-AZO film. The electron donating amine group in the SAM molecule could have strong interaction with Al^{3+} ions of the AZO film that lead to form the highly oriented AZO film. The electron donating group, —NH_2 SAM modified uv-PET-AZO film showed the good crystallinity and reduction in resistivity when compared with electron withdrawing group, —CN SAM modified uv-PET-AZO film. The lowest resistivity of 1.1×10^{-3} Ω cm was obtained for AZO film deposited on uv-PET substrate modified by —NH_2 SAM at optimized conditions. This study suggests a novel low temperature approach to improve the crystallinity of AZO film on PET by modulate the surface dipole moment of PET substrate, which could be extend to improve the qualities of other inorganic films when depositing on polymeric substrates.

References

[1] H. Kim, C. Gilmore, J. Horwitz, A. Pique, H. Murata, G. Kushto, R. Schlaf, Z. Kafafi, D. Chrisey, Transparent conducting aluminum-doped zinc oxide thin films for organic light-emitting devices, Appl. Phys. Lett. 76 (3) (2000) 259–261.
[2] J.-M. Kim, P. Thiyagarajan, S.-W. Rhee, Deposition of Al-doped ZnO films on polyethylene naphthalate substrate with radio frequency magnetron sputtering, Thin Solid Films 518 (20) (2010) 5860–5865.
[3] X. Jiang, F.L. Wong, M.K. Fung, S.T. Lee, Aluminum-doped zinc oxide films as transparent conductive electrode for organic light-emitting devices, Appl. Phys. Lett. 83 (9) (2003) 1875–1877.
[4] R. Cebulla, R. Wendt, K. Ellmer, Al-doped zinc oxide films deposited by simultaneous rf and dc excitation of a magnetron plasma: relationships between plasma parameters and structural and electrical film properties, J. Appl. Phys. 83 (2) (1998) 1087–1095.
[5] E.-G. Fu, D.-M. Zhuang, G. Zhang, Z. ming, W.-F. Yang, J.-J. Liu, Properties of transparent conductive ZnO:Al thin films prepared by magnetron sputtering, Microelectron. J. 35 (4) (2004) 383–387.
[6] R. Wen, L. Wang, X. Wang, G.-H. Yue, Y. Chen, D.-L. Peng, Influence of substrate temperature on mechanical, optical and electrical properties of ZnO:Al films, J. Alloys Compd. 508 (2) (2010) 370–374.
[7] D.-K. Kim, H.-B. Kim, Dependence of the properties of sputter deposited Al-doped ZnO thin films on base pressure, J. Alloys Compd. 522 (2012) 69–73.
[8] A.A. Al-Ghamdi, O.A. Al-Hartomy, M. El Okr, A.M. Nawar, S. El-Gazzar, F. El-Tantawy, F. Yakuphanoglu, Semiconducting properties of Al doped ZnO thin films, Spectrochim. Acta Part A 131 (2014) 512–517.
[9] K.D. Harris, A.L. Elias, H.-J. Chung, Flexible electronics under strain: a review of mechanical characterization and durability enhancement strategies, J. Mater. Sci. 51 (6) (2016) 2771–2805.
[10] T. Sekitani, U. Zschieschang, H. Klauk, T. Someya, Flexible organic transistors and circuits with extreme bending stability, Nat. Mater. 9 (12) (2010) 1015–1022.
[11] C.-A. Fustin, A.-S. Duwez, Dithioesters and trithiocarbonates monolayers on gold, J. Electron Spectrosc. Relat. Phenom. 172 (1–3) (2009) 104–106.
[12] N. Saran, K. Parikh, D.-S. Suh, E. Muñoz, H. Kolla, S.K. Manohar, Fabrication and characterization of thin films of single-Walled carbon nanotube bundles on flexible plastic substrates, J. Am. Chem. Soc. 126 (14) (2004) 4462–4463.
[13] C.H. Tseng, C.H. Huang, H.C. Chang, D.Y. Chen, C.P. Chou, C.Y. Hsu, Structural and optoelectronic properties of Al-doped zinc oxide films deposited on flexible substrates by radio frequency magnetron sputtering, Thin Solid Films 519 (22) (2011) 7959–7965.
[14] Z.L. Pei, X.B. Zhang, G.P. Zhang, J. Gong, C. Sun, R.F. Huang, L.S. Wen, Transparent conductive ZnO:Al thin films deposited on flexible substrates prepared by direct current magnetron sputtering, Thin Solid Films 497 (1–2) (2006) 20–23.
[15] S. Fernández, A. Martínez-Steele, J.J. Gandía, F.B. Naranjo, Radio frequency sputter deposition of high-quality conductive and transparent ZnO:Al films on polymer substrates for thin film solar cells applications, Thin Solid Films 517 (10) (2009) 3152–3156.
[16] Akio Suzuki; Tatsuhiko Matsushita; Naoki Wada; Yoshiaki Sakamoto; Masahiro Okuda, Transparent conducting Al-doped ZnO thin films prepared by pulsed laser deposition, Jpn. J. Appl. Phys. 35 (1A) (1996) L56.
[17] M. Miyake, H. Fukui, T. Hirato, Preparation of Al-doped ZnO films by aqueous solution process using a continuous circulation reactor, Phys. Status Solidi (A) 209 (5) (2012) 945–948.
[18] R. Chandramohan, T.A. Vijayan, S. Arumugam, H.B. Ramalingam, V. Dhanasekaran, K. Sundaram, T. Mahalingam, Effect of heat treatment on microstructural and optical properties of CBD grown Al-doped ZnO thin films, Mater. Sci. Eng. B 176 (2) (2011) 152–156.
[19] H. Hagendorfer, K. Lienau, S. Nishiwaki, C.M. Fella, L. Kranz, A.R. Uhl, D. Jaeger, L. Luo, C. Gretener, S. Buecheler, Y.E. Romanyuk, A.N. Tiwari, Highly transparent and conductive ZnO: Al thin films from a low temperature aqueous solution approach, Adv. Mater. 26 (4) (2014) 632–636.
[20] T.T.T. Vo, Y.-H. Ho, P.-H. Lin, Y. Tai, Control of growth mode and crystallinity of aluminium-doped zinc oxide thin film at room temperature by self-assembled monolayer assisted modulation on substrate surface energy, CrystEngComm 15 (34) (2013) 6695–6701.
[21] Y. Tai, J. Sharma, H.-C. Chang, T.V.T. Tien, Y.-S. Chiou, Self-assembled monolayers induced inter-conversion of crystal structure by vertical to lateral growth of aluminium doped zinc oxide thin films, Chem. Commun. 47 (6) (2011) 1785–1787.
[22] W. Chen, T.J. McCarthy, Layer-by-layer deposition: a tool for polymer surface modification, Macromolecules 30 (1) (1997) 78–86.
[23] J. Xiang, P. Zhu, Y. Masuda, K. Koumoto, Fabrication of self-assembled monolayers (SAMs) and inorganic micropattern on flexible polymer substrate, Langmuir 20 (8) (2004) 3278–3283.
[24] W.A. Zisman, Relation of the equilibrium contact angle to liquid and solid constitution, Adv. Chem. 43 (1964) 1–51.
[25] E. Hoque, J.A. DeRose, P. Hoffmann, B. Bhushan, H.J. Mathieu, Alkylperfluorosilane self-assembled monolayers on aluminum: a comparison with alkylphosphonate self-assembled monolayers, J. Phys. Chem. C 111 (10) (2007) 3956–3962.
[26] S. Kobayashi, T. Nishikawa, T. Takenobu, S. Mori, T. Shimoda, T. Mitani, H. Shimotani, N. Yoshimoto, S. Ogawa, Y. Iwasa, Control of carrier density by self-assembled monolayers in organic field-effect transistors, Nat. Mater. 3 (5) (2004) 317–322.
[27] Y. Tanaka, K. Kanai, Y. Ouchi, K. Seki, Role of interfacial dipole layer for energy-level alignment at organic/metal interfaces, Org. Electron. 10 (5) (2009) 990–993.
[28] M.F. Calhoun, J. Sanchez, D. Olaya, M.E. Gershenson, V. Podzorov, Electronic functionalization of the surface of organic semiconductors with self-assembled monolayers, Nat. Mater. 7 (1) (2008) 84–89.
[29] J. Kong, H. Dai, Full and modulated chemical gating of individual carbon nanotubes by organic amine compounds, J. Phys. Chem. B 105 (15) (2001) 2890–2893.
[30] H. Kang, S. Hong, J. Lee, K. Lee, Electrostatically self-assembled nonconjugated polyelectrolytes as an ideal interfacial layer for inverted polymer solar cells, Adv. Mater. 24 (22) (2012) 3005–3009.